J. Phys. A: Math. Gen. **29** (1996) 5297–5311. Printed in the UK

Renormalization of correlations and spectra of a strange non-chaotic attractor

Ulrike Feudel†, Arkady Pikovsky† and Antonio Politi‡

† Max-Planck-Arbeitsgruppe 'Nichtlineare Dynamik', Universität Potsdam, Potsdam, Germany
‡ Istituto Nazionale di Ottica, Firenze, Italy, INFM and INFN Sezione di Firenze

Received 4 January 1996

Abstract. We study a simple nonlinear mapping with a strange nonchaotic attractor characterized by a singular continuous power spectrum. We show that the symbolic dynamics is exactly described by a language generated from a suitable inflation rule. We derive renormalization transformations for both the power spectrum and the autocorrelation function, thus obtaining a quantitative description of the scaling properties. The multifractal nature of the spectrum is also discussed.

1. Introduction

The autocorrelation function and the power spectrum are standard tools in the investigation of complex dynamical processes. Given a discrete-time, stationary process with unit variance $[x_t]$, the autocorrelation function $C(\tau)$ is defined as

$$C(\tau) = \langle x_t x_{t+\tau} \rangle.$$

The behaviour of the autocorrelation function enables one to recognize periodic and chaotic motions: in the former case $C(\tau)$ is periodic with $C(T) = C(0) = 1$, where T is the period of the oscillations; in the latter, $C(\tau)$ usually decreases exponentially for increasing τ†. The autocorrelation function of a quasiperiodic process is quasiperiodic too, returning arbitrarily close to 1.

Periodic, chaotic and quasiperiodic motions have different spectral properties. By defining the Fourier transform of the sequence $[x_t]$ as

$$s(\omega, T) = T^{-1/2} \sum_{t=1}^{T} x_t e^{i2\pi\omega t} \tag{1}$$

the power spectrum can be represented as

$$P(\omega) = \lim_{T\to\infty} \langle |s(\omega, T)|^2 \rangle.$$

In the periodic case, the power spectrum consists of δ-peaks at the harmonics of the basic frequency, while in the chaotic case, the power spectrum is continuous. For a quasiperiodic motion with incommensurate basic frequencies ω_1, ω_2, the power spectrum generally contains all the combinational frequencies $n\omega_1 + m\omega_2$.

† A mixture of periodic and chaotic motion eventually gives a periodic correlation function, never returning to the value 1.

0305-4470/96/175297+15$19.50

The above classification, although widespread in the literature (see e.g. [1]), is not complete. Indeed, as is known from the mathematical theory of spectral measures [2, 3], in general a spectrum is composed of a discrete, an absolutely continuous, and a singular continuous component. The discrete component consists of δ peaks, the absolutely continuous component is a broad band spectrum having finite density, and the singular continuous component is a fractal: it sits on a set of Lebesgue measure zero, but its peaks are weaker than δ-functions. The autocorrelation function corresponding to a singular continuous spectrum does not usually decay to zero, but also does not return to 1. One can say that systems having such correlations lie between order and chaos. Recently, singular continuous spectra have been reported for a number of physical systems [4–8].

In this paper we study a simple model of strange non-chaotic attractor that was numerically shown in [9] to exhibit a singular continuous spectrum. Strange non-chaotic attractors (SNA) typically appear in quasiperiodically forced nonlinear systems [10, 11]. They are non-chaotic in the sense that there is no sensitive dependence on initial conditions (the Lyapunov exponent is negative), while they are strange in the geometrical sense, exhibiting a fractal structure in the phase space. The goal of this paper is to describe quantitatively this spectrum by means of symbolic dynamics and renormalization.

In section 2 we define the basic SNA model studied in [9–11], discussing the skew product structure which was first introduced in the context of ergodic theory. Here, we also briefly review scaling properties of correlations and spectra, observed in [9]. In section 3 we give a symbolic description of the SNA and derive a scaling transformation for the spectrum which allows us to describe its multifractal properties. A similar approach has been applied to the spectrum of the Feigenbaum attractor in [12], and to singular continuous spectra in [4, 5]. In section 4, a renormalization transformation for the autocorrelation function is proposed, to explain its self-similarity.

2. Basic model

2.1. Strange nonchaotic attractor and skew product

We consider the two-dimensional mapping

$$x_{t+1} = 2\lambda \tanh(x_t) \sin 2\pi\theta_t \tag{2}$$

$$\theta_{t+1} = \theta_t + \xi \bmod 1. \tag{3}$$

Equation (3) is the circle map which produces, in the case of irrational ξ, a quasiperiodic force acting on the variable x. It was demonstrated in [10] that for $\lambda > 1$ the system (2), (3) has an SNA. For further investigations of this model see [11, 13].

Spectral properties of the variable x have been studied numerically in [9], presenting indications that the spectrum is singular continuous. In fact, the autocorrelation function and the power spectrum of a signal deriving from a dynamical system depend on the observable. In [9] the 'natural' observable x has been used. However, the quantitative analysis can be extremely simplified if instead of referring to x, the discrete observable y defined as

$$y_t = -\operatorname{sign}(x_t) \tag{4}$$

is investigated. This observable takes values -1 and 1 only, and can be considered as a symbolic representation of the dynamics given by (2), (3) (the remaining part $\tilde{x}_t = x_t/y_t$ is an upper semicontinuous function of θ_t, as has been recently shown in [13]). We can write the evolution equation for y as

$$y_{t+1} = y_t \Phi(\theta_t) \tag{5}$$

where the function Φ is

$$\Phi(\theta) = \begin{cases} -1 & \text{if } 0 \leqslant \theta < \frac{1}{2} \\ 1 & \text{if } \frac{1}{2} \leqslant \theta < 1. \end{cases} \tag{6}$$

The systems (2), (3) and, equivalently, (5), (3) are known in the mathematical literature as 'skew-product' models [14]. In a skew-product system, a variable satisfying a self-contained equation (here θ) is used to force a second dynamical system without any feedback. Spectral properties of the skew product (5), (3) have been studied in [15–17, 3], where it has been proved that the spectrum is singular continuous.

Quantitative properties of the spectrum depend on the choice of the frequency ξ. For the case ξ being the reciprocal of the golden mean $\xi = (\sqrt{5}-1)/2$, the autocorrelation function and the spectrum have remarkable self-similarity which we explain below quantitatively on the basis of a renormalization group approach.

2.2. Scaling properties of correlations and spectra

In this section we describe the scaling properties of correlations and spectra, as they appear from direct numerical simulations [9]. The autocorrelation function of the sequence (4) is presented in figure 1. It has peaks with amplitude ≈ 0.55 at all even Fibonacci numbers. Around such peaks, the correlation function exhibits a similar behaviour:

$$C(F_{3n+\tau}) \approx C(F_{3n})C(\tau) \tag{7}$$

as one can see in figure 2.

It is useful to consider the spectrum as a 'process' and plot it for different lengths of the time series. In figure 3, one can see the typical peaks of fractal measures, which are expected to grow as a power law,

$$|s(\omega, T)|^2 \sim T^{\gamma(\omega)}$$

where $\gamma < 1$. This can be directly seen from figure 4, for some frequencies ω. The exponents γ have been numerically obtained in [9]. In the next section, we compare such numbers with the prediction of the renormalization group approach.

3. Renormalization of the spectrum

3.1. Construction of the symbolic sequence

The variable y_t provides a symbolic representation of the process x_t. In this section we describe the self-similar properties of the symbolic signal y_t. There are at least two types of recursive relations yielding self-similar symbolic sequences: inflation and concatenation rules. Starting from an inflation rule for an auxiliary sequence, we derive a concatenation rule for it, to finally obtain a concatenation rule for the sequence y_t.

Consider first a sequence $[z_t]$ of symbols $(-1, 1)$ generated according to the rule $z_t = \Phi(\theta_t)$, where θ_t obeys (3) and the function Φ is given by (6). According to [18], z_t is a symbolic representation of the circle map having rotation number ξ, with the coding angle $\frac{1}{2}$. In [5] it has been shown that the symbolic trajectory of $\theta_0 = 0$ can be produced from the following inflation rule:

$$\begin{aligned} A &\to T(A) = CAC \\ B &\to T(B) = CACCA \\ C &\to T(C) = CACBA \end{aligned} \tag{8}$$

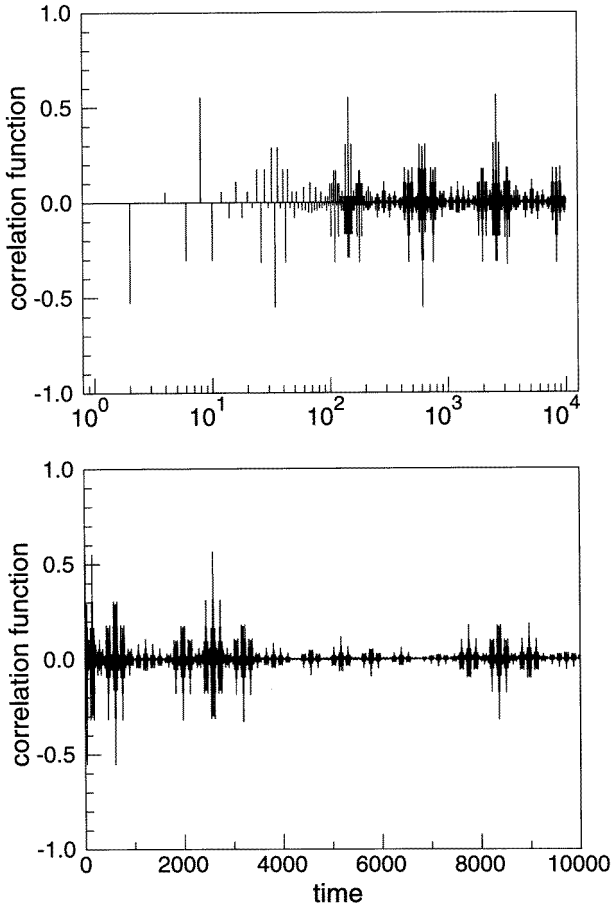

Figure 1. The autocorrelation function of the sequence $[y_t]$ in linear (bottom panel) and logarithmic (top panel) scales.

in terms of the three symbols A, B, C. The sequence z_t is obtained by repeatedly applying (8) to the initial sequence $z_1 = C$ and by eventually setting $A = B = -1$, $C = 1$. We describe below an equivalent procedure to obtain z_t from a concatenation rule.

The length of the sequence obtained in a finite number n of steps is naturally expressed by the Fibonacci numbers F_n ($F_1 = F_2 = 1$, $F_n = F_{n-1} + F_{n-2}$). Let us denote with Z_n the sequence $\{z_t\}$ with length F_n. It is convenient to define three sequences

$$U_k = Z_{3k+2} \qquad V_k = Z_{3k+3} \qquad W_k = Z_{3k+4}.$$

The initial conditions for the application of the rule (8) are

$$U_0 = C \qquad V_0 = CA \qquad W_0 = CAC.$$

Now we can derive the recursive relations for U, V, W. Applying the inflation rule to the U_0, V_0, W_0 we get

$$U_{k+1} = T^{k+1}(C) = T^k(CACBA) = T^k(CAC)T^k(BA) = W_k W_{k-1} V_{k-1} W_{k-1} \tag{9}$$

$$V_{k+1} = T^{k+1}(CA) = T^{k+1}(C)T^k(CAC) = U_{k+1} W_k \tag{10}$$

$$W_{k+1} = T^{k+1}(CAC) = T^{k+1}(CA)T^{k+1}(C) = V_{k+1} U_{k+1}. \tag{11}$$

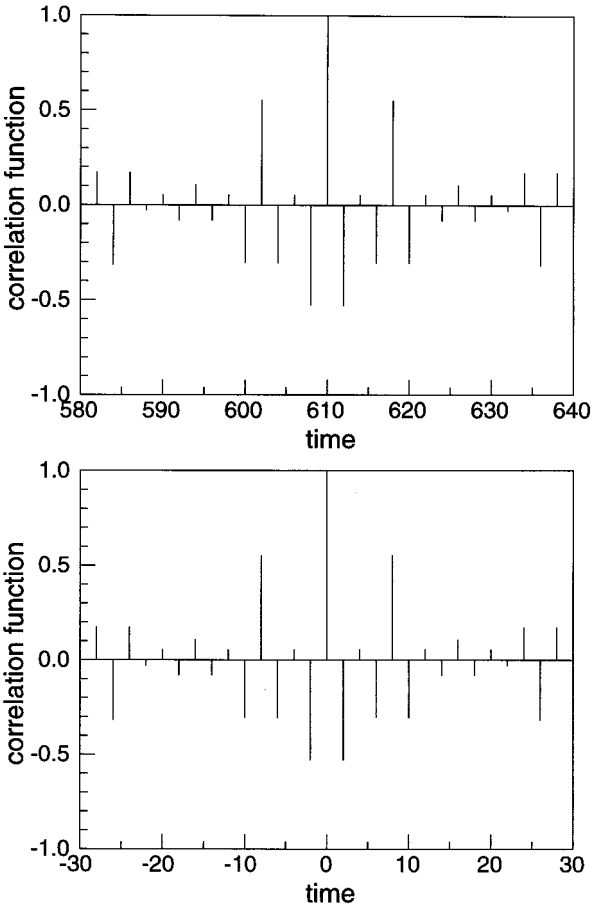

Figure 2. Part of the autocorrelation function near one of the main peaks at $\tau = 610$ (normalized by $C(610)$), and the corresponding part of the original autocorrelation function near the origin.

From (9), it is seen that the computation of U_1 requires the knowledge of both W_{-1} and V_{-1}, which are not defined. The problem can be solved by adding $U_1 = CACBA$ to the initial conditions. There is an alternative way to write the expression for U_{k+1}:

$$U_{k+1} = V_k W_k' \tag{12}$$

where the prime means that the last symbol of the string is inverted. To see this, note that for $k = 0$

$$U_1 = CACBA \qquad \text{and} \qquad V_0 W_0 = CACAC$$

so that (12) is valid for $k = 0$. These sequences differ only in the last two elements. Because

$$AC \to CACCACBA \qquad BA \to CACCACAC$$

for any k, these sequences differ only in the last two elements. After substitution $A = B = -1$, $C = 1$ we get (12).

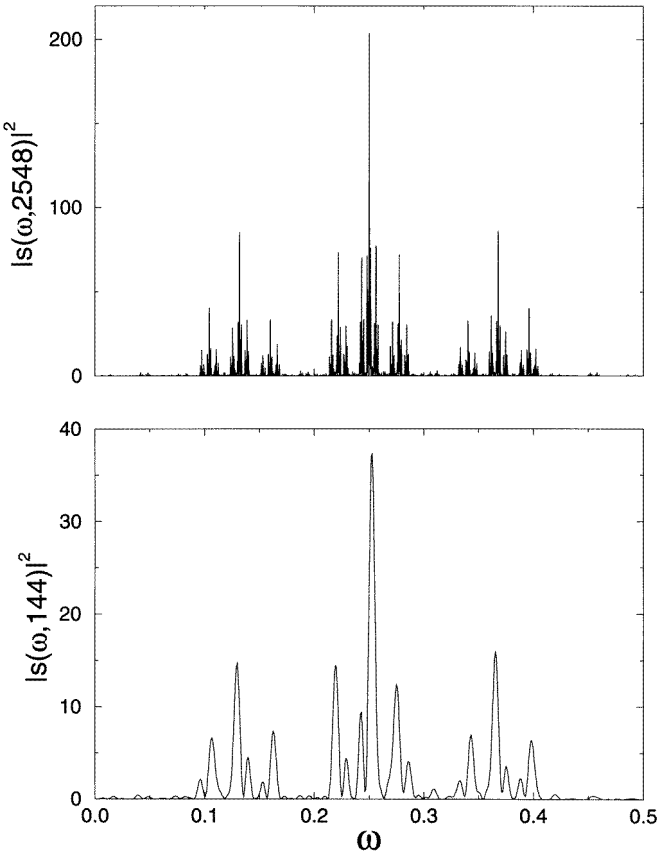

Figure 3. Finite-time power spectra for $T = 144$ and $T = 2584$.

With reference to the sequence of interest, Z_n, the concatenation rule can be written as

$$Z_{n+1} = \begin{cases} Z_n Z_{n-3} Z_{n-4} Z_{n-3} = Z_{n-1} Z'_n & \text{if } n = 3k+1,\ k \geqslant 2 \\ Z_n Z_{n-1} & \text{otherwise.} \end{cases} \tag{13}$$

Accordingly, one can say that the recursive relation for the symbolic sequence $[z_t]$ has 'period 3' (in terms of the Fibonacci numbers).

Consider now the process (5), which can be rewritten as

$$y_t = y_{t-1} z_t = \prod_1^t z_i \qquad y_0 = 1$$

and let us derive a concatenation rule for the sequence $[y_k]$. Again, we denote the sequence $[y_k]$ of length F_n by Y_n. It is convenient to write explicitly the dependence of Y_n on the initial element y_0: $Y_n(y_0)$. We want to calculate $Y_n(1)$ (note that $Y_n(-1) = \overline{Y_n}$, where the bar denotes the inversion of all elements in the sequence).

Let us denote with $R(Z)$ the product of all elements in a finite sequence Z. We show by induction that, for $k \geqslant 1$,

$$R(U_k) = (-1)^k \qquad R(V_k) = (-1)^{k+1} \qquad R(W_k) = -1.$$

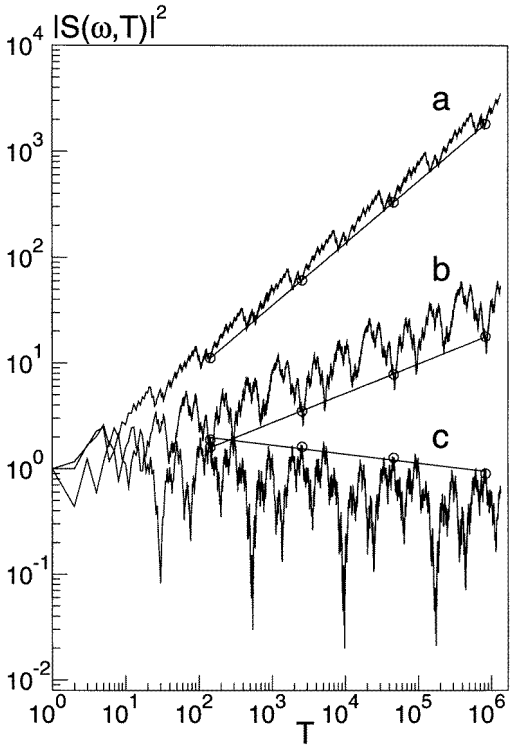

Figure 4. Spectral sums for the frequencies (*a*) 1/4, (*b*) $(3+\xi)/5$ and (*c*) $\xi/4$. A linear fit for the encircled points gives slopes 0.588, 0.277, and −0.085, respectively (compare with the data for γ in table 1). The origin of these numbers, as well as the periodic structure of the curves, is explained in section 3.

For $k = 1$ this is checked directly. For $k > 1$ from (9)–(11) we have

$$R(U_{k+1}) = R(V_{k-1})R(W_k) = (-1)^{k+1}$$
$$R(V_{k+1}) = R(U_{k+1})R(W_k) = (-1)^{k+2}$$
$$R(W_{k+1}) = R(V_{k+1})R(U_{k+1}) = -1$$

which completes the proof. We can also write these relations as

$$R(Z_{6k}) = R(Z_{6k+2}) = 1 \qquad R(Z_{6k+1}) = R(Z_{6k+3}) = R(Z_{6k+4}) = R(Z_{6k+5}) = -1. \tag{14}$$

Now we apply this result to concatenation rule (13):

$$Y_{n+1}(1) = \begin{cases} Y_n(1)Y_{n-3}[R(Z_n)]Y_{n-4}[R(Z_n)R(Z_{n-3})] & \\ \quad \times Y_{n-3}[R(Z_n)R(Z_{n-3})R(Z_{n-4})] & \text{if } n = 3k+1 \\ Y_n(1)Y_{n-1}[R(Z_n)] & \text{if } n = 3k+2 \\ Y_n(1)Y_{n-1}[R(Z_n)] & \text{if } n = 3k+3. \end{cases}$$

Taking into account (14), we get

$$\begin{aligned} Y_{6k+3} &= Y_{6k+2}Y_{6k+1} \\ Y_{6k+4} &= Y_{6k+3}\overline{Y}_{6k+2} \\ Y_{6k+5} &= Y_{6k+4}\overline{Y}_{6k+1}Y_{6k}Y_{6k+1} \\ Y_{6k+6} &= Y_{6k+5}\overline{Y}_{6k+4} \\ Y_{6k+7} &= Y_{6k+6}Y_{6k+5} \\ Y_{6k+8} &= Y_{6k+7}\overline{Y}_{6k+4}Y_{6k+3}\overline{Y}_{6k+4}. \end{aligned} \tag{15}$$

Formula (15) is the desired concatenation rule for the symbolic sequence $[y_t]$. This should be supplemented with the initial condition $Y_2 = -Y_1 = 1$, and Y_0 equal to the empty string. Notice that the recursive relation for the sequence $[y_t]$ has 'period 6'—the period doubled in comparison to that for $[z_t]$, because of the additional change of sign.

With the help of (12), the third and the sixth of the recursive relations (15) can be rewritten in a more compact way:

$$\begin{aligned} Y_{6k+5} &= Y_{6k+3}\overline{Y}'_{6k+4} \\ Y_{6k+8} &= Y_{6k+6}Y'_{6k+7}. \end{aligned} \tag{16}$$

These relations are certainly less elegant in that they involve a partial manipulation of the structure of some sequence, but they lead to a simpler renormalization transformation for the power spectrum.

3.2. Renormalization transformation for the spectrum

The non-normalized Fourier transform of the sequence $Y_n = [y_1, \ldots, y_{F_n}]$ is defined as

$$S_n(\omega) = \sum_{k=1}^{F_n} y_k \mathrm{e}^{\mathrm{i}2\pi k\omega}. \tag{17}$$

The normalized finite-time Fourier transform (1) introduced in (17) is related to $S_n(\omega)$ in the following way:

$$s(\omega, F_n) = \frac{1}{F_n^{1/2}} S_n(\omega). \tag{18}$$

Concatenation rule (15) modified as in (16) allows us to obtain a recursive relation for $S_n(\omega)$. By properly taking into account the phases, one obtains

$$\begin{aligned} S_{6k+3} &= S_{6k+2} + \mathrm{e}^{\mathrm{i}\phi_{6k+2}} S_{6k+1} \\ S_{6k+4} &= S_{6k+3} - \mathrm{e}^{\mathrm{i}\phi_{6k+3}} S_{6k+2} \\ S_{6k+5} &= S_{6k+3} - \mathrm{e}^{\mathrm{i}\phi_{6k+3}} S_{6k+4} - 2\mathrm{e}^{\mathrm{i}\phi_{6k+5}} \\ S_{6k+6} &= S_{6k+5} - \mathrm{e}^{\mathrm{i}\phi_{6k+5}} S_{6k+4} \\ S_{6k+7} &= S_{6k+6} + \mathrm{e}^{\mathrm{i}\phi_{6k+6}} S_{6k+5} \\ S_{6k+8} &= S_{6k+6} + \mathrm{e}^{\mathrm{i}\phi_{6k+6}} S_{6k+7} + 2\mathrm{e}^{i\phi_{6k+8}} \end{aligned} \tag{19}$$

where, for the sake of brevity, we omit the ω-dependence, while

$$\phi_n \equiv 2\pi F_n \omega$$

satisfies

$$\phi_n = \phi_{n-1} + \phi_{n-2} \pmod{2\pi}. \tag{20}$$

The initial conditions are

$$S_0 = 0 \qquad S_1 = -\mathrm{e}^{\mathrm{i}2\pi\omega} \tag{21}$$

and

$$\phi_0 = 0 \qquad \phi_1 = 2\pi\omega. \tag{22}$$

The asymptotic behaviour of S_n gives the growth rate of the spectral component at a given frequency ω. It depends crucially on the evolution of of ϕ. Mapping (20) is Arnold's cat map: it has chaotic trajectories and an everywhere dense set of periodic orbits. If ϕ is eventually attracted to a periodic orbit having period m (i.e. if the initial point lies on the stable manifold of this orbit), then system (19) can be seen as a periodically driven linear map. Accordingly, when the evolution is monitored every Kth iteration, where K is the least common multiple of m and 6, we find that it is described by a time-independent† linear map acting on a two-dimensional space (in fact, the updating of S_{n+1} always requires the knowledge of S_n and S_{n-1} only). Here, we see the advantage of using representation (16), since equation (15) would have led to a 3D map instead.

It is easily seen that the determinant of the homogeneous part of transformation (19) has modulus one in each of the six steps. Accordingly, volumes are conserved and the moduli of the two eigenvalues of each periodic orbit are the inverse of each other. Therefore, the growth rate Λ of S_n, i.e. the largest Lyapunov exponent of map (19), cannot be smaller than 0. Accordingly, the normalized spectral component $|s(\omega, T)|^2$ grows with time T as $|s(\omega, T)|^2 \sim T^{\gamma}$, where

$$\gamma = 2\frac{\Lambda}{\log(1/\xi)} - 1. \tag{23}$$

A power-law behaviour is precisely the growth rate that has been numerically observed in [9], as illustrated in figure 4.

To determine the frequencies that yield such a self-similar behaviour, we have to find the intersections of the line of initial conditions with the stable manifold of the periodic orbits of mapping (20) in the plane $(x, y) \equiv (\phi_{n-1}, \phi_n)$. The stable manifold of the periodic orbit passing through (x_0, y_0) is the line $(x - x_0) = -\xi(y - y_0)$. The frequencies that correspond to an evolution along such a manifold are determined by imposing $x = 0$ and $y = 2\pi\omega$,

$$\omega = \frac{x_0}{2\pi\xi} + \frac{y_0}{2\pi} + N + M/\xi$$

for all possible integers M and N. The scaling behaviour around all these frequencies is determined by the Lyapunov exponent of the periodic trajectory induced in the plane (S_{n-1}, S_n) by the orbit stemming from x_0, y_0‡. The numerical results for some short-period orbits are listed in table 1, where it can be seen that the minimum expansion rate $\Lambda = 0$ is exactly attained in some cases, while the fastest growth rate is observed for a period-6 orbit.

3.3. Multifractal properties of the spectrum

In this section we discuss the multifractal properties of the spectrum. In fact, the latter can be interpreted as a measure on the interval $0 \leqslant \omega < 1$ and, in turn, the thermodynamic

† Here, we mean the renormalization time.

‡ It is important to note that the same periodic trajectory in the plane (x, y) can give rise to different eigenvalues depending on the phase difference between that orbit and the period-6 of spectral transformation (19).

Table 1. The eigenvalues δ of the renormalization transformation for the spectrum (19) for some periodic orbits of (20). The corresponding indices $\gamma(\omega)$ (23) are compared with the numerical data in [9].

Period m	LCM K	x_0	y_0	ω	Λ	γ	γ from [9]
3	6	1/2	1/2	$1/2+\xi/2$	0	-1	
3	6	0	1/2	$\xi/2$	0	-1	-1
3	6	1/2	0	1/2	0	-1	-1
4	12	3/5	1/5	$(3+\xi)/5$	0.307 12	0.276 44	
4	12	2/5	4/5	$(2+4\xi)/5$	0.307 12	0.276 44	
4	12	1/5	2/5	$(1+2\xi)/5$	0.112 38	−0.532 93	
4	12	4/5	3/5	$(4+3\xi)/5$	0.112 38	−0.532 93	
5	30	1/11	3/11	$(1+3\xi)/11$	0.172 73	−0.282 12	
				All period-5 cycles have the same eigenvalues			
6	6	1/4	0	1/4	0.382 07	0.587 96	0.58
6	6	3/4	0	3/4	0.382 07	0.587 96	0.58
6	6	0	1/4	$\xi/4$	0.219 49	−0.087 75	−0.02

formalism for fractal measures (see, e.g. [19]) applied. By dividing the interval $0 \leqslant \omega < 1$ into L subintervals with size $\varepsilon = 1/L$ and after denoting their measures with p_k, we can write the coarse-grained partition function as

$$\Gamma(\varepsilon, q) = \sum_{1}^{L} p_k^q \tag{24}$$

the growth rate of which,

$$\Gamma(\varepsilon, q) \sim \varepsilon^{\tau(q)} \tag{25}$$

defines the function $\tau(q)$. The generalized dimensions D_q and the corresponding $f(\alpha)$-spectrum are linked by a standard Legendre transform

$$\begin{aligned} &D_q = \tau(q)/(q-1) \\ &f(\alpha) = q\alpha - \tau(q) \qquad \alpha = \mathrm{d}\tau/\mathrm{d}q. \end{aligned} \tag{26}$$

In our case, the coarse-grained spectral measure can be qualitatively interpreted as the finite-time Fourier transform (17). The frequency resolution after n renormalization steps is F_n^{-1}, so that it is natural to assume $\varepsilon = F_n^{-1}$ and $p_k = |s_n(\omega_k)|^2\varepsilon$. By substituting such assumptions in (24), (25) one obtains

$$\sum_{1}^{F_n} p_k^q \approx \varepsilon^{q-1} \int_0^1 |s_n(\omega)|^{2q}\,\mathrm{d}\omega \sim F_n^{-\tau(q)}$$

which implies

$$\int_0^1 |s_n(\omega)|^{2q}\,\mathrm{d}\omega \sim F_n^{q-1-\tau(q)}. \tag{27}$$

This relation allows one to determine the multifractal properties of the spectral measure directly from the iteration of (19). We find that $D_0 = 1$, an equality that follows from the absence of holes in the spectrum, while $D_1 \approx 0.75$, and $D_2 \approx 0.65$. The whole $f(\alpha)$-spectrum is reported in figure 5.

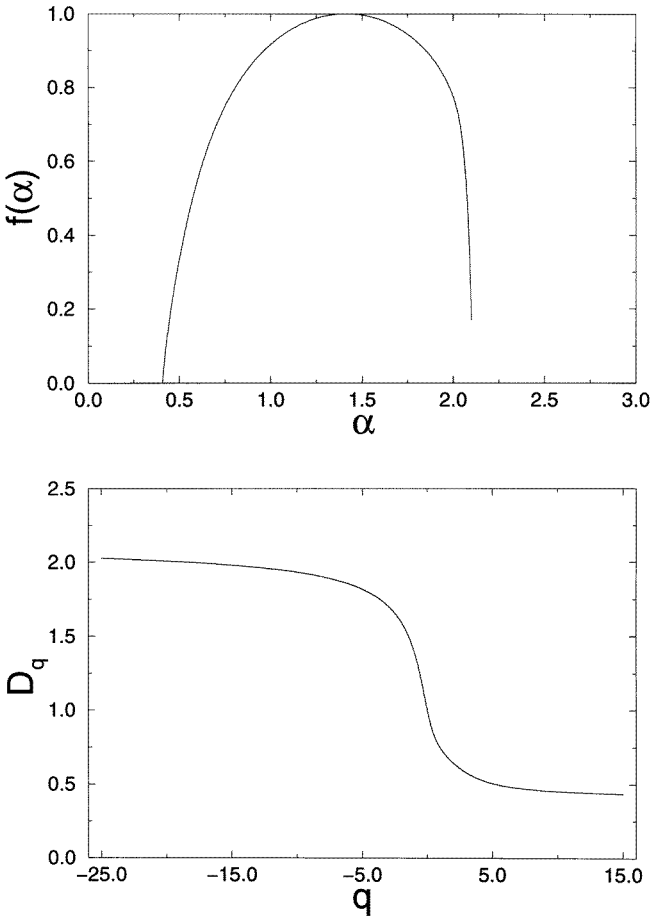

Figure 5. The generalized dimensions D_q and the $f(\alpha)$-spectrum of the fractal power spectrum (figure 3).

In fact, formula (27) can be used to obtain the spectrum of the growth rates of the spectral components, averaged over different frequencies ω. Indeed, upon assuming a finite T, (27) can be rewritten as

$$\int_0^1 |s(\omega, T)|^{2q}\, \mathrm{d}\omega \sim T^{\sigma(q)}. \tag{28}$$

After Legendre transforming [19], one obtains the spectrum of generalized Lyapunov exponents γ,

$$g(\gamma) = \sigma(q) - q\gamma \qquad \gamma = \mathrm{d}\sigma/\mathrm{d}q.$$

A similar relation holds for Λ as well; here we are naturally led to introduce γ as it refers to the growth rate of the normalized spectral component with $\ln T$, as it is understood in (28) (let us recall that Λ, instead, refers to the unnormalized component versus the number of steps in the renormalization group transformation). By noticing that

$$\sigma(q) = q - 1 - \tau(q)$$

and comparing with (26), we obtain a relation between the distribution of growth rates and the $f(\alpha)$ spectrum

$$\alpha = 1 - \gamma \qquad f(\alpha) = 1 + g(\gamma).$$

In particular, the smallest α value corresponds to the largest Lyapunov exponent. We have found $\alpha_{\min} \approx 0.408$ while, according to the table, $(1 - \gamma_{\max}) = (1 - \gamma(\frac{1}{4})) \approx 0.412$.

The agreement between the two approaches is not so good for large α's (small Lyapunov exponents). In fact, the spectral tail seen in figure 5 above $\alpha = 2$ cannot be reproduced by any periodic orbit, since the determinant of transformation (19) has modulus 1. Accordingly, the smallest possible γ value is -1 (see (23)), which corresponds to $\alpha = 2$. By investigating different approximations $|S_n|$ of the power spectrum, we have found that the low-density regions (responsible for the anomalous scaling behaviour) vary along the ω-axis in a rather irregular manner with n, confirming that such points have nothing to do with the fixed points of the renormalization transformation.

However, we failed to find a convincing explanation for the spectral tail. On the one hand, it is possible that it is a finite-size effect orginating from strong and long-period fluctuations (in $\ln T$) during the growth of the spectral components (as is suggested by the curves in figure 4). On the other hand, it is not unreasonable to trace back the difference to a lack of hyperbolicity of the mapping. In fact, we should notice that while the two transformations (19), (22) can be separately considered as linear mappings, they are altogether nonlinear (the nonlinearity arises in the multiplicative factors containing the phase information)†. Because of the nonlinearity, stable and unstable manifolds are not everywhere transverse (see the marginally stable orbits of period 3). In such a case, it is known that different thermodynamic approaches may give rise to different results (see, for instance [20], where the role of homoclinic tangencies is discussed in the Hènon map). Moreover, even without invoking non-hyperbolicity, since stable and unstable manifolds change direction in the phase space (S_{n-1}, S_n), it is possible that the initial condition of recursive relation (21) could be (almost) aligned along the stable direction of some periodic orbit, thus giving rise to an exponent γ smaller than -1.

4. Renormalization of the autocorrelation function

In this section we study the scaling properties of the autocorrelation function of y_t,

$$C(t) = \langle y_n y_{n+t} \rangle.$$

From

$$y_n = \prod_{k=1}^{n} z_k$$

it follows that

$$C(t) = \left\langle \prod_{k=1}^{n} z_k \prod_{l=1}^{n+t} z_l \right\rangle = \left\langle \prod_{k=1}^{n} z_k^2 \prod_{l=n+1}^{n+t} z_l \right\rangle = \langle y_t \rangle.$$

The ergodicity property of the mapping implies that the average in the above equation can be computed as an integral over all possible initial conditions in the circle map (3)

$$C(t) = \int_0^1 \prod_{k=1}^{t} \Phi(\theta + k\xi)\, \mathrm{d}\theta \tag{29}$$

† The nonlinearity is precisely the mechanism responsible for a non-trivial multifractal spectrum, otherwise all periodic orbits would exhibit the same scaling behaviour.

the variable y being a function of the initial phase,

$$y_t(\theta) = \prod_{k=1}^{t} \Phi(\theta + k\xi).$$

From this representation, it can be seen that $C(t)$ vanishes for odd t. Indeed, since Φ is periodic with period 1, we can arbitrarily change the range of k in (29),

$$C(t) = \int_0^1 \prod_{k=k_0}^{t+k_0-1} \Phi(\theta + k\xi)\, \mathrm{d}\theta.$$

By fixing $k_0 = -m$ for $t = 2m + 1$, one obtains

$$C(2m+1) = \int_0^1 \Phi(\theta) \prod_{k=1}^{m} \Phi(\theta + k\xi)\Phi(\theta - k\xi)\, \mathrm{d}\theta = 0$$

since the integral of the odd function vanishes.

Consider now the scaling properties of the function $y_t(\theta)$. We take this function at Fibonacci times $t = F_n$. For $R_n(\theta) \equiv y_{F_n}(\theta)$, we can write

$$R_n(\theta) = \prod_{k=1}^{F_n} \Phi(\theta + k\xi) = \prod_{k=1}^{F_{n-1}} \Phi(\theta + k\xi) \prod_{k=F_{n-1}+1}^{F_n} \Phi(\theta + k\xi) = R_{n-1}(\theta) R_{n-2}(\theta + F_{n-1}\xi).$$

By taking into account that $F_{n-1}\xi = F_{n-2} - (-\xi)^{n-1}$, one obtains

$$R_n(\theta) = R_{n-1}(\theta) R_{n-2}(\theta - (-\xi)^{n-1}).$$

The explicit 'time'-dependence which makes the above equation non-autonomous can be removed by rescaling θ, i.e. by introducing $Q_n(y) = R_n(y(-\xi)^n)$. The new function satisfies the recursive relation

$$Q_n(y) = Q_{n-1}(-\xi y) Q_{n-2}(\xi^2 y + \xi) \tag{30}$$

which represents the renormalization transformation underlying the structure of the correlation function (see also [21–23], where this relation appeared in different contexts). In fact, it is numerically seen that the functional mapping exhibits a period-6 solution, $Q_l = Q_{l+6}$, with some symmetry properites such as, for example, $Q_{3(2l+1)} = -Q_{6l}$: a plot of this solution over two periods is reported in figure 6.

The correlation function can be represented as

$$C(F_n) = \langle y_{F_n} \rangle = \langle R_n \rangle = \langle Q_n \rangle.$$

For $n = 3l + 1$ and $n = 3l + 2$, the Fibonacci numbers F_n are odd and $\langle Q_n \rangle = 0$, while for $n = 3l$ we observe

$$C(F_{6l}) = -C(F_{3(2l+1)}) \approx 0.55.$$

The function $Q_n(y)$ has a characteristic period in y of order 1 which corresponds to a characteristic scale of order $\xi^n \ll 1$ in θ for $R_n(\theta)$. With reference to $y_t(\theta)$ for $t = F_n + \tau$, we can write

$$y_{F_n+\tau}(\theta) = R_n(\theta) \prod_{k=1}^{\tau} \Phi(\theta + k\xi + F_n\xi).$$

If $|\tau| \ll F_n$, the two terms in the right-hand side oscillate on different scales. Therefore, if $\langle R_n \rangle \neq 0$, i.e. if $n = 3l$, the average involved in the definition of $C(t)$ factorizes,

$$C(F_n + \tau) = \int_0^1 y_{F_n+\tau}(\theta)\, \mathrm{d}\theta \approx \langle R_n \rangle \int_0^1 y_\tau(\theta + F_n\xi)\mathrm{d}\theta = C(F_n)C(\tau).$$

This relation accounts for the numerically observed self-similar nature of the autocorrelation function.

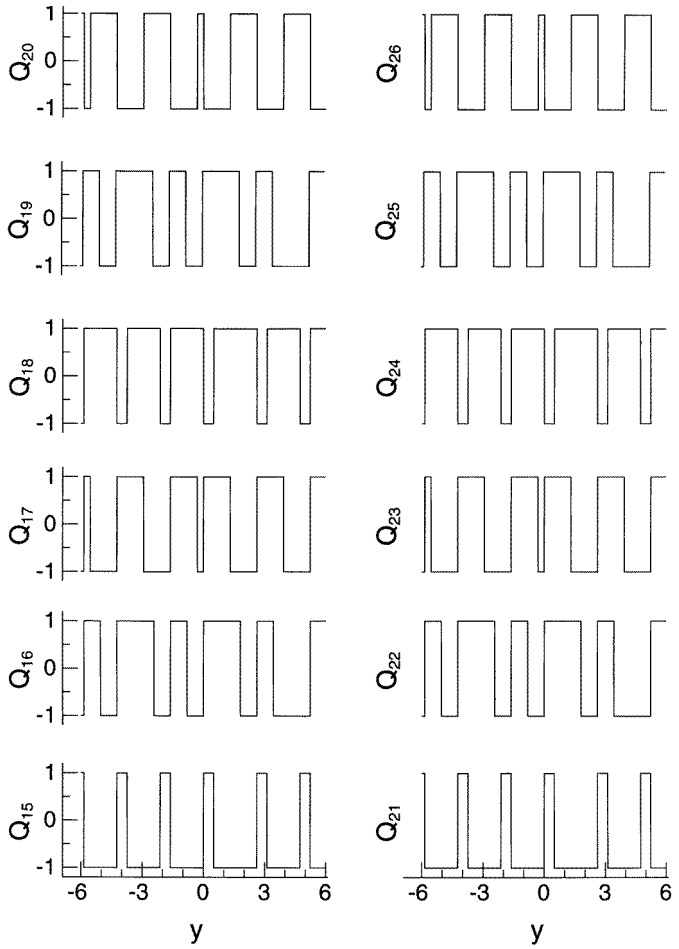

Figure 6. Period-6 solution of the renormalization transformation (30).

5. Conclusion

We have developed a renormalization approach yielding a quantitative description of the fractal power spectrum and of the correlation function of a strange non-chaotic attractor (3). The characterization of the power spectrum is made possible by the self-similarity of the symbolic representation of the dynamics, which allows us to construct a recursive transformation for the spectrum. Peaks in the spectrum correspond to periodic orbits of this transformation, and their strength is measured by the corresponding eigenvalues. For the autocorrelation function, we obtain a functional renormalization equation, and we observe numerically that it evolves towards a period-6 orbit. We have also demonstrated how the self-similarity of the autocorrelation function follows from the properties of such a solution.

Our approach makes essential use of the self-similar structure of the external periodic forcing, hidden in the reciprocal golden-mean rotation-number. A generalization to other irrationals exhibiting periodic continuous fractions is straightforward; consideration of 'arbitrary' irrational numbers needs further investigation.

Acknowledgments

We thank J Kurths, S Kuznetsov, U Smilansky and M Zaks for useful discussions. This work, initiated during the INFM-FORUM activity for Theoretical Physics in Firenze, has been partly performed during the 1995 ISI Workshop on 'Complexity and Chaos': AP and AP thank the Institute for Scientific Interchange (Torino) for their hospitality. The support of the German–Italian VIGONI program is also acknowledged.

References

[1] Argyris J, Faust G and Haase M 1994 *An Exploration of Chaos* (Amsterdam: North-Holland)
[2] Cornfeld I P, Fomin S V and Sinai Ya G 1982 *Ergodic Theory* (New York: Springer)
[3] Queffélec M 1987 *Substitution Dynamical Systems—Spectral Analysis (Springer Lecture Notes in Mathematics 1294)* (Berlin: Springer)
[4] Aubry A, Godrèche C and Luck J M 1987 *Europhys. Lett.* **4** 639
[5] Aubry S, Godrèche C and Luck J M 1988 *J. Stat. Phys.* **51** 1033
[6] Artuso R *et al* 1994 *Int. J. Mod. Phys.* B **8** 207
[7] Cheng Z, Savit R and Merlin R 1988 *Phys. Rev.* B **37** 4375
[8] Godrèche C and Luck J M 1990 *J. Phys. A: Math. Gen.* **23** 3769
[9] Pikovsky A and Feudel U 1994 *J. Phys. A: Math. Gen.* **27** 5209
[10] Grebogi C, Ott E, Pelikan S and Yorke J A 1984 *Physica* **13D** 261
[11] Pikovsky A and Feudel U 1995 *Chaos* **5** 253
[12] Kuznetsov S P and Pikovsky A S 1989 *Phys. Lett.* **140A** 166
[13] Keller G 1995 *Preprint* 21/95, University of Erlangen-Nürenberg
[14] Anzai H 1951 *Osaka Math. J.* **3** 83
[15] Oseledec V I 1966 *Sov. Math. Dokl.* **7** 776
[16] Katok A B and Stepin A M 1967 *Russ. Math. Surv.* **22** 77
[17] Riley G W 1978 *J. London Math. Soc.* **17** 152
[18] Siegel R M, Tresser Ch and Zettler G 1992 *Chaos* **2** 473
[19] Crisanti A, Paladin G and Vulpiani A 1993 *Products of Random Matrices in Statistical Physics* (Berlin: Springer)
[20] Grassberger P, Badii R and Politi A 1988 *J. Stat. Phys.* **51** 135
[21] Kuznetsov S, Pikovsky A and Feudel U 1995 *Phys. Rev.* E **51** R1629
[22] Feudel U, Pikovsky A S and Zaks M A 1995 *Phys. Rev.* E **51** 1762
[23] Ketoja J A and Satija I I 1995 *Phys. Rev. Lett.* **75** 2762